Metallography, Microstructure, and Analysis (2023) 12:171–186
https://doi.org/10.1007/s13632-023-00937-3

PEER-REVIEWED PAPER

Metallographic Investigation of the Bronze Sword from Vértesszőlős

Szilvia Gyöngyösi[1] · Géza Szabó[2] · Péter Barkóczy[3] · Julianna Cseh[4]

Received: 10 October 2022 / Revised: 31 December 2022 / Accepted: 24 January 2023 / Published online: 23 February 2023

Abstract
The area of Vértesszőlős was a populated area during the wide period of the Bronze Age. Artifacts from different cultures, and among them, many bronze objects were found. Most are ornaments, but tools and weapons have also been unearthed. The weapons found are a fragment of a sword, a blade tip fragment, and a dagger. The primary purpose of the study is the metallographic analysis of the objects to reveal the characteristics of their alloys and the manufacturing technique. It is also important from the point of view of identifying the basic copper alloy groups based on many test results. The study of the microstructure also provides new knowledge for this, and it also allows to determine the manufacturing technique. The purpose of the tests shall be to establish a detailed metallographic examination and compositional and manufacturing information.

Keywords Bronze age · Sword · Metallography · Carpathian basin

Introduction

The settlements and burial site of Vértesszőlős (Northern-Hungary, close to Tatabánya) (Fig. 1) were settlements and a burial place used for a long time in the Bronze Age [1]. Its excavation and investigation provide an important contribution to the research of the Bronze Age in the Carpathian Basin [2]. The rich collection of artifacts contains many metal objects, which are being investigated within the framework of a complex research program [3]. In addition, several Bronze Age sites provide an opportunity to evaluate the results in broader context [4]. Therefore, the rich Bronze Age metalworking of the Carpathian Basin is the basis of several research programs [5, 6].

Vértesszőlős is a settlement belonging to the collection area of the Museum of Tatabánya (Komárom-Esztergom County). It is located between Tata and Tatabánya, at the eastern foot of the Gerecse mountains, on the banks of the Által-ér. It is a strategic geographical position, as the first secure crossing of the Danube River southwards, it has also been exploited by many prehistoric cultures. Among them are the populations of the entire Bronze Age period of The Mako (Early Bronze Age) [7], Encrusted Pottery (Middle Bronze Age) [8], and the Tumulus and Urnfield cultures (Late Bronze Age)[9, 10].

The site is located directly South-West of the village, in the area between the main road No. 1 and the Budapest-Győr-Vienna railway line, on terrace 2 of the Által-ér (Fig. 1). The most important results of the probing excavations conducted by János László in 2008, and in 2009, led by Gabriella A. Pál: i, the settlement detail of the Makó culture, ii, the cemetery details of the Transdanubian Encrusted Pottery Culture, iii, the details of the settlements of the Late Bronze Age (Urnfield Culture) and the Roman and Árpád Periods, iv, the settlement and cemetery objects (Tumulus Culture) that can be dated to the end of the Middle Bronze Age and the beginning of the Late Bronze Age and can be linked to the early stage of the Tumulus Culture. During the

This invited article is part of a special topical issue of the journal *Metallography, Microstructure, and Analysis* on Archaeometallurgy. The issue was organized by Dr. Patricia Carrizo, National Technological University–Mendoza Regional, and Dr. Omid Oudbashi, Art University of Isfahan and The Metropolitan Museum of Art, on behalf of the ASM International Archaeometallurgy Committee.

✉ Péter Barkóczy
fembarki@uni-miskolc.hu; peter.barkoczy@gmail.com

1 Institute of Mechanical Engineering, University of Debrecen, Debrecen, Hungary

2 Wosinsky Mór Museum, Szekszárd, Hungary

3 Faculty of Materials Engineering, University of Miskolc, Miskolc, Hungary

4 Tatabánya Museum, Tatabánya, Hungary

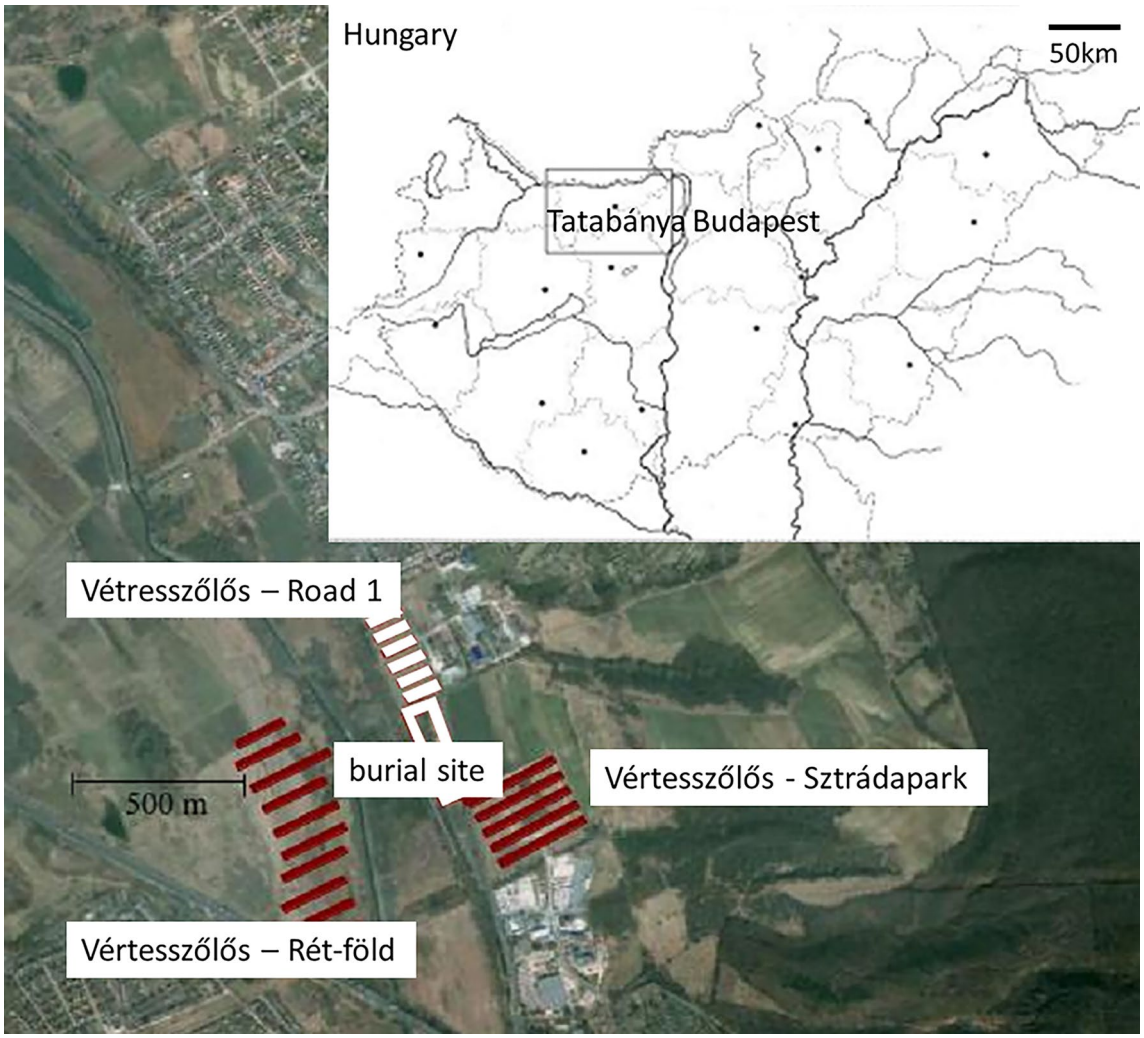

Fig. 1 The location of Vértesszolos burial site in Hungary and in the present Village of Vértesszolos

excavations, the depo and the mixed surface between the objects were also continuously examined with metal-finding instruments, thanks to which many metal objects (mostly bronze and Roman) were found [1].

Instrumental examination of bronze objects is an important tool for the research of the Bronze Age [11, 12]. The examination of certain important, valuable objects [13, 14] or the comprehensive examination of deposited object groups and hoards [15–17] all contribute to the knowledge of the metalworking of a particular area and era [18, 19] or to the exploration of the relationships between areas [20, 21] migrations [22, 23]. Bronze weapons and swords play an important role in this research [24, 25]. The number of swords found is significantly less than that of utility and ornaments, nevertheless their role makes them a special focus in all studies [26].

Classical metallographic practice can be traced in the study of Bronze Age metal artefacts [27]. However, the place, method and sample size of sampling are critical to the value and appearance of the object [28]. Modern restoration techniques and procedures provide more and more possibilities in this area as well, although the possibilities are certainly limited compared to modern metallography practice [29]. The largest possible sample should be used to determine the most information. Care should be taken, both at sampling and during the evaluation phase, to ensure that the sample and results remain representative [30].

It is important to know the typical alloys and their effects due to the abovementioned constraint when examining bronze alloys [31]. In addition, the basic context of copper contemporary metallurgy is required to know [32]. In the Carpathian Basin, tin bronze alloys occur most often although a considerable amount of arsenic can also be found in addition to tin [33]. In addition, based on previous studies, it is important to study the amount of iron, nickel, antimony, and silver in the metal. The ratio of these alloying elements

is suitable for grouping the raw copper alloy. If sufficient data are available, the groups can even be linked to a metal source area [34]. Isotopic studies of lead and tin can also be of considerable help in this [35, 36]. Of course, as more and more data are collected, the more objects are examined in detail, the more accurate results will become. Of course, the composition of the alloys also affects their strength [40–43]. To assess it, it is also necessary to know the state of the alloy (as cast, deformed, annealed), which can be revealed by metallographic examination.

In the case, when a sample cannot be taken from the object, it is also interesting information about the material and its structure. More and more non-destructive methods are being used to examine metal finds [37–39]. Thus, the evaluation of the results leads to more and more detailed information about the object within the limits given by the methods. Although metallographic examination provides the most detailed set of results, when there is no possibility of sampling, modern techniques are required for more important information.

For the above reasons, it is important to carry out a detailed metallographic examination of the objects of the Vértesszőllős site. The examination program includes a bronze sword fragment, a blade fragment of a sword, and a bronze dagger. The examination of each objects adds an important contribution to the results and evaluations of the previous studies [1, 3]. The primary purpose of the study is a detailed metallographic examination to reveal the alloy and the manufacturing technique. The basic methods of this study are optical microscopy and SEM–EDS analysis. Both methods are given the possibility to gather more information about objects and compare objects based on their raw material and manufacturing. During sampling, it was necessary to cut the fragmentary parts under the guidance of specialists of course. But in each case, due to the nature of the object, a representative sample for the manufacturing technique of the object was taken.

The mentioned objects are shown in Fig. 2. The assumption was used that the blade fragment is part of the fragmentary sword, the two objects belong together. Both their size and shape allowed this to be assumed. Investigations have shown that the two objects, however, are a part of two separate swords. The dagger was also classified as a well-preserved object suitable for examination. However, studies have shown that due to the strong effect of corrosion, only partial information is obtained. The article summarizes the test results.

Materials and Methods

A detailed metallographic examination was carried out on the bronze sword of Vértesszőlős. The sword itself is fragmented, one larger piece is the grip and part of the blade. The point of the blade is missing. The whole sword was made of one piece, which can be seen on Fig. 2a. There were rivets in the cross-guard part, which either had a decorative function or fixed the unseen, missing part of the grip and cross guard to the sword. No traces of this missing part were found. However, three rivets remained in the cross guard. The dimensions of the sword are as follows: the blade is 210 mm long and 35–48 mm wide, the grip is 67 mm long and 16–22 mm wide.

The blade fragment, a tip is 51 mm long and 19 mm wide (Fig. 2b). The outlook of the blade fragment is quite similar to the blade of the sword described above. It could be assumed this blade fragment is the missing part of the sword.

The grip plate was sampled from two places which is a large and fragmented part of the sword. Sampling from the blade part was not permitted, however, the tip fragment was

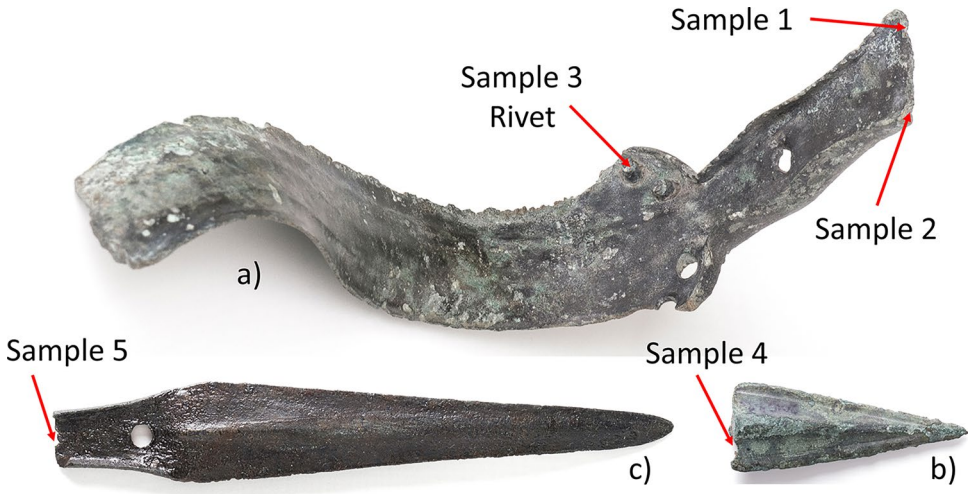

Fig. 2 The photos were taken from the examined artifacts: (**a**) bronze sword with a rivet, (**b**) a blade fragment of a bronze sword, (**c**) bronze dagger

sampled. A rivet was removed from the sword, which could be studied in its entire cross-section.

No samples were taken from the blade of the sword, but the blade fragment was sampled as the supposed broken tip of the sword. In this case, as in other artifacts, it had to be considered that sampling meant the least visible damage on the object. A fragmentary part of the object provided an opportunity for this.

In addition to the sword, a fragment of a dagger was also unearthed during the excavation. The dimension of the blade is: 140 mm in length and 20 mm in width (Fig. 2c). The length of the handle is 25 mm while its width is 12 mm. The sample taken from the dagger blade would have significantly affected the object and its visual appearance in the exhibition. As a result, a sample was taken from the grip plate. With this sampling the nature of the sword and the dagger remained comparable.

Sampling was carried out carefully by sawing to avoid significant heating of the objects. The location of the samples is shown in Fig. 2. The sample size was chosen to provide sufficient depth below the corrosion, determined by the estimated thickness of the corrosion layer. However, the dimension of the objects creates a limit. Tests were carried out on the cut metallic surface. Samples, after grinding (SiC) and polishing (1 µm diamond), are etched with an aqueous solution of potassium bichromate. Optical microscopic images were taken with Zeiss AxioImager M1m microscope in bright field and polarized illumination. Local composition analysis and chemical element distribution mapping were performed using a Bruker EDS probe mounted on Hitachi 4300 CFE SEM equipment.

Results and Discussion

Blade Fragment of a Bronze Sword

The sample taken from the blade fragment of the bronze sword has a dendritic structure (Fig. 3). The sword was made by casting. The secondary dendrite arm spacing is ~ 25 µm. The secondary arm spacing and the whole microstructure is uniform in the examined section of the sample (Fig. 3b).

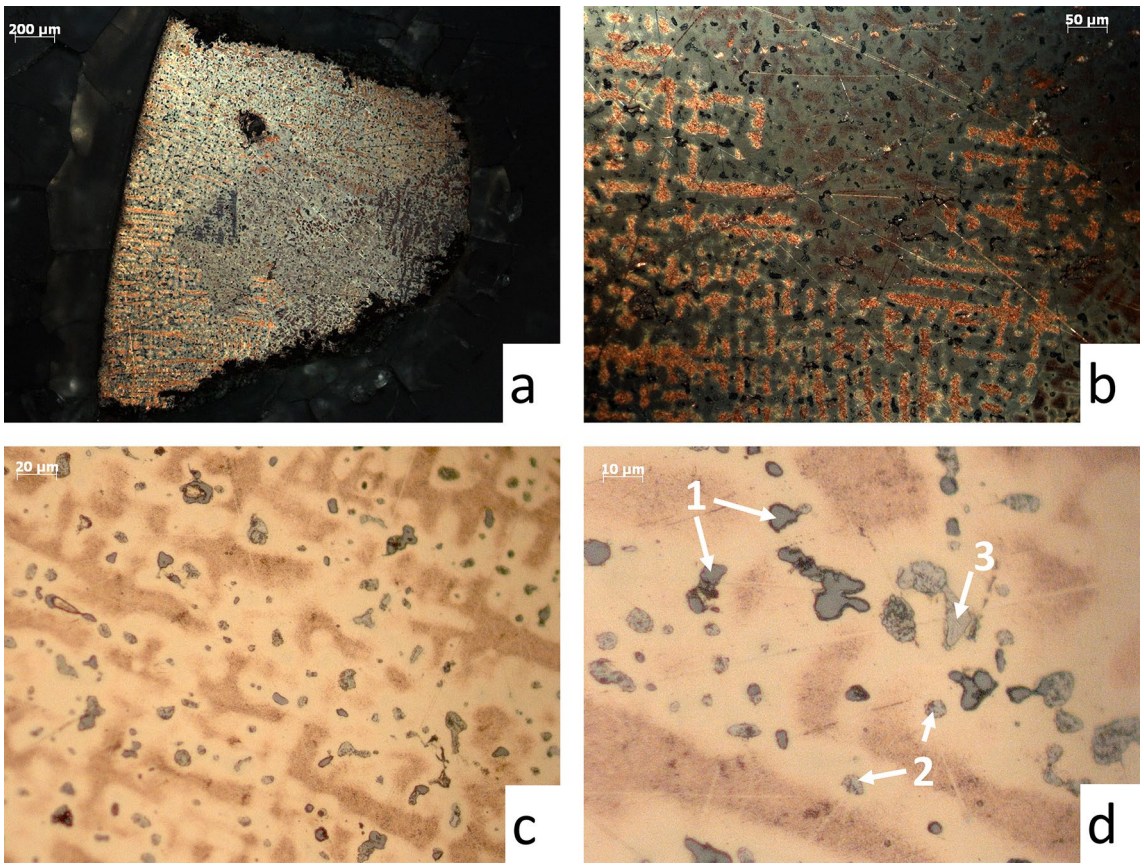

Fig. 3 Optical micrographs of the sample taken from the blade fragment of a bronze sword. The photos show the microstructure of the sample in different magnifications. Photos (**a**) and (**b**) were made in polarized light illumination. Dendritic microstructure can be seen on these (**a**, **b**) micrographs. Photos (**c**) and (**d**) were made in bright field illumination. The traces of micro segregation in the dendrite arms (**c**) suggest relatively rapid cooling during solidification. More inclusion can be seen in the microstructure in high magnification (**d**)

Etching reveals a significant micro segregation in the bright-field images (Fig. 3c). The traces of micro-segregation and dendrite arm spacing indicate a relatively fast cooling. Comparing this with the geometry and dimensions of the tip of the sword, it is an excepted result.

High magnification optical microscopy images reveal a significant number of small-sized inclusions. The diameter range of these inclusion is from 1 to 2 µm to 15 µm. At least three types of inclusions can be distinguished based on their colour and morphology in the optical microscopic images: a) larger (5–10 µm) dark grey, mostly compact inclusions are copper sulphide inclusions (1 in Fig. 3d); b) spherical light grey inclusions in the small size range are lead droplets (2 in Fig. 3d); c) larger, more polyhedral light grey inclusions are intermetallic compounds with a high tin content (3 in Fig. 3d).

SEM–EDS study was performed on the same sample that was examined with an optical microscope to investigate these phases. The preparation of the sample was not supplemented by an extra additional step. The average composition of the blade fragment was estimated based on the EDS spectrum measured in different area (Fig. 4a, b). The results are summarized in Table 1. The average composition was measured in typical fields on the sample. The results show that the blade fragment is bronze with medium tin content (~5 wt.%). In addition, a relatively high nickel content can be measured. In addition to nickel, the concentration of arsenic, silver and antimony suggests a nickel-containing version of the tetrahedrite group as a source of ore. Among the alloys of artifacts found in the Carpathian Basin, this is a characteristic type. Archaeological analyzes link the source of this type of alloy, specifically the copper base of it to the Alps [4, 11]. The lead content is extremely inhomogeneous, which is not surprising to see in the copper-lead alloys. High lead content was determined (~4.5 wt.%). The addition of this amount of lead helps the mold filling during casting as there is liquid phase in the alloy at lower temperatures during the solidification. Such a high lead content could be beneficial for proper manufacturing, conversely it is modified the mechanical properties of course. The literature investigated the effect of lead content on an as cast copper alloy [40, 43] containing 6 wt.% tin. The hardness of the alloy was measured at ~70HV1. 2 wt.% added lead increased hardness by 19% and 10 wt.% lead reduced it by 15%. The measured

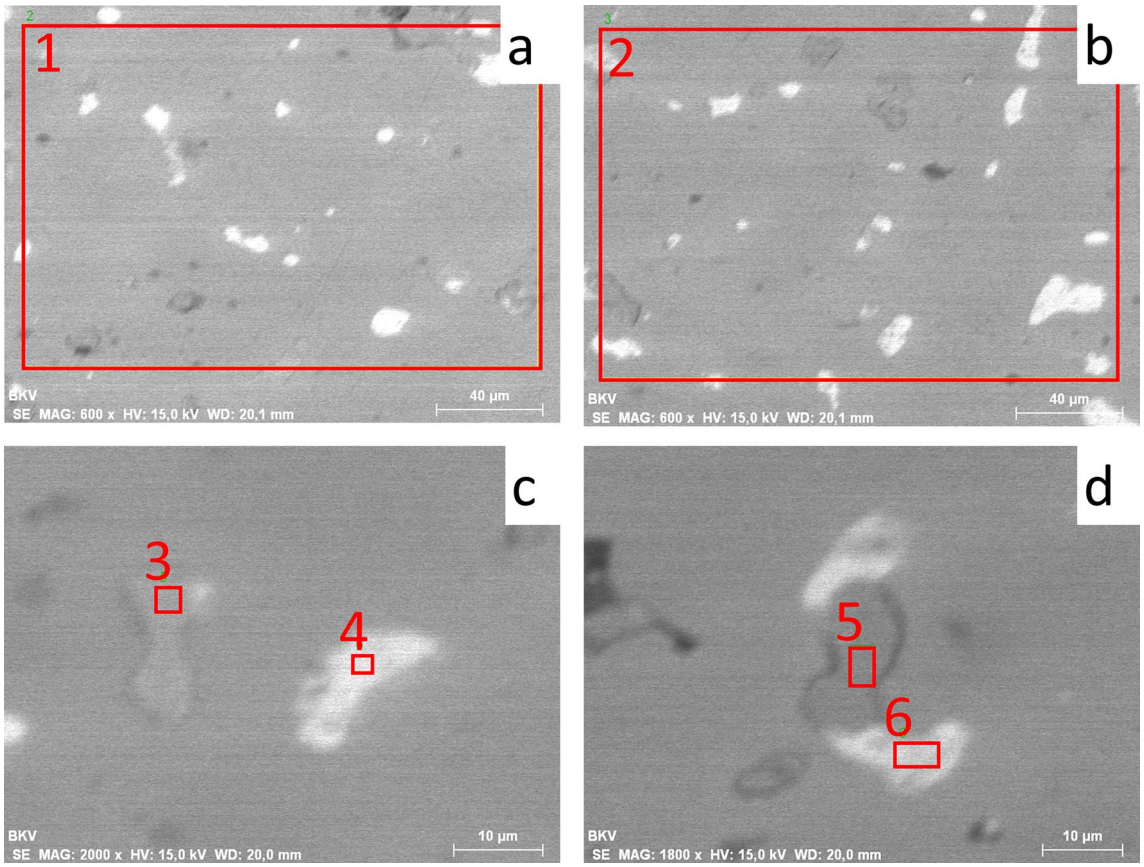

Fig. 4 The SEM micrographs of the blade fragment of a bronze sword. Areas of the EDS analysis of the average chemical composition (**a**, **b**) and the places of the local analysis of different phases are shown on the photos (**c**, **d**)

Table 1 The results of EDS analysis of the blade fragment of a bronze sword

Location	C	O	Mg	Al	Si	P	S	Mn	Fe	Ni	Cu	As	Ag	Sn	Sb	Pb
1	7.9	2.4	0.1	0.1		0.1				1.7	71.7	0.4	0.7	4.7	0.7	9.6
2	6.4	1.5		0.1		0.2	0.1			1.9	81.4	0.7	0.7	5.4	0.9	0.7
3	8.1	3.2	0.1					0.8	1.0	2.0	52.8	0.1	0.9	21.8	4.6	4.6
4	2,9	7,0		0.1							5.6	0.6	5.6	1.0	1.3	75.8
5	9.9	2.1		0.2	0.1		14.3				64.3			2.6	0.9	5.7
6	9.6	2.3		0.2	0.1						4.7			1.1	1.2	80.8

The areas of analysis are shown on Fig. 4

4.5w% represents nearly the same hardness as the hardness of the alloy without any added lead. However, it does not reduce the mechanical properties to such an extent that the sword is not suitable for its weapon function.

Analysis points 4 and 6 show extremely high lead content (Fig. 4c and d). Copper does not dissolve lead in their alloy either in a melt or solid state. For this reason, lead is found in the microstructure in an almost pure state as solidified droplets. The sulfur content of point 5 is extremely high (Fig. 4d), which indicates that the inclusion is copper sulfide. The content of tin, antimony and lead in the inclusion is probably a consequence of the excitation of the metal matrix. An extremely high content of tin is measured in the composition of point 3, close to the composition of the β compound phase of copper-tin alloys. This suggests that the intermetallic phase formed because of micro segregation. These SEM–EDS studies have revealed these 3 types of inclusions and intermetallic phases.

Sample 1 of the Bronze Sword

Two samples were taken from the broken grip plate of the bronze sword. One is from the edge of the grip. The sample was prepared for examination using the same method as for the blade fragment. Optical microscopic images are shown in Fig. 5. A duplex, recrystallized grain structure can be seen (Fig. 5a and b) where the difference between the diameters of large and small grains is large. In addition to large (~ 150 µm) grains, small (~ 25 µm) grains are also visible in the microstructure of the sample (Fig. 5b). The nature of the particles and the thermal twins in the grains show that these formed during a recrystallization process due to annealing after a metal forming process (Fig. 5c). The duplex grain structure suggests a slight plastic deformation (less than 50% in reduction) of the examined volume at elevated temperature. The nature of the sword suggests casting instead of forging. This small extent of plastic deformation could be made either when the sword was taken out of the mould or during the forming of the final shape of the grip. If plastic deformation was intended, it was carried out while the sword was still warm, at a temperature where recrystallization takes place even after a slight deformation (> = 400 °C) [42, 43].

The prepared section is heavily affected by corrosion. Thinner-thicker corrosion products are situated on the grain boundaries (denoted by 1–2 on Fig. 5d). However, the mostly spherical, dark grey sulphide inclusions in the optical microscopic images (Figs. 5e and f) are clearly separated from the corrosion products. To verify this and determine the composition, SEM–EDS tests were carried out. The images are shown in Fig. 6, and the results of the composition measurement are shown in Table 2.

The composition of the sword is significantly different from the blade fragment. The tin content is high (~ 8 wt.%) but lead content is not detectable. Although the base copper alloy seems similar in its nature, antimony in the sword material could not be detected by SEM–EDS analysis. In addition, the content of nickel, arsenic and silver is also lower than in case of blade fragment. Compared to the difference in tin content, the quality of the basic copper alloy is close to each other except for the antimony content. Previous classification of other artifacts by raw material revealed that the existence of the antimony is important. The basic composition of the inclusions was checked using local analyses. The copper and tin content within the grains was also measured as the basic values. Indeed, the dark grey inclusions of optical microscopy are copper sulphide inclusions. The element map of the dendritic inclusion shown in the optical microscopic image of Fig. 5f is shown in Fig. 7. These types of inclusions were enclosed in the microstructure of the metal during the smelting of the copper. The tiny light phase incorporated into the inclusion is lead. The lead inclusions generally occur mostly in association with sulphide inclusions [44, 45]. The number and the size of lead phases explains why the average composition analysis does not show this low lead content.

Figure 6 shows SEM images taken from the sample. The noted area and points show the places of chemical analysis. The inside of the grain is the inclusion and the phase on the grain boundary are also analyzed at several points. The phase at the grain boundaries is a corrosion product. This is suggested by local analysis showing a significant increase in oxygen content compared to measurement inside the grains. With a small sulphur content, phosphorus and iron also appear. Arsenic and significant

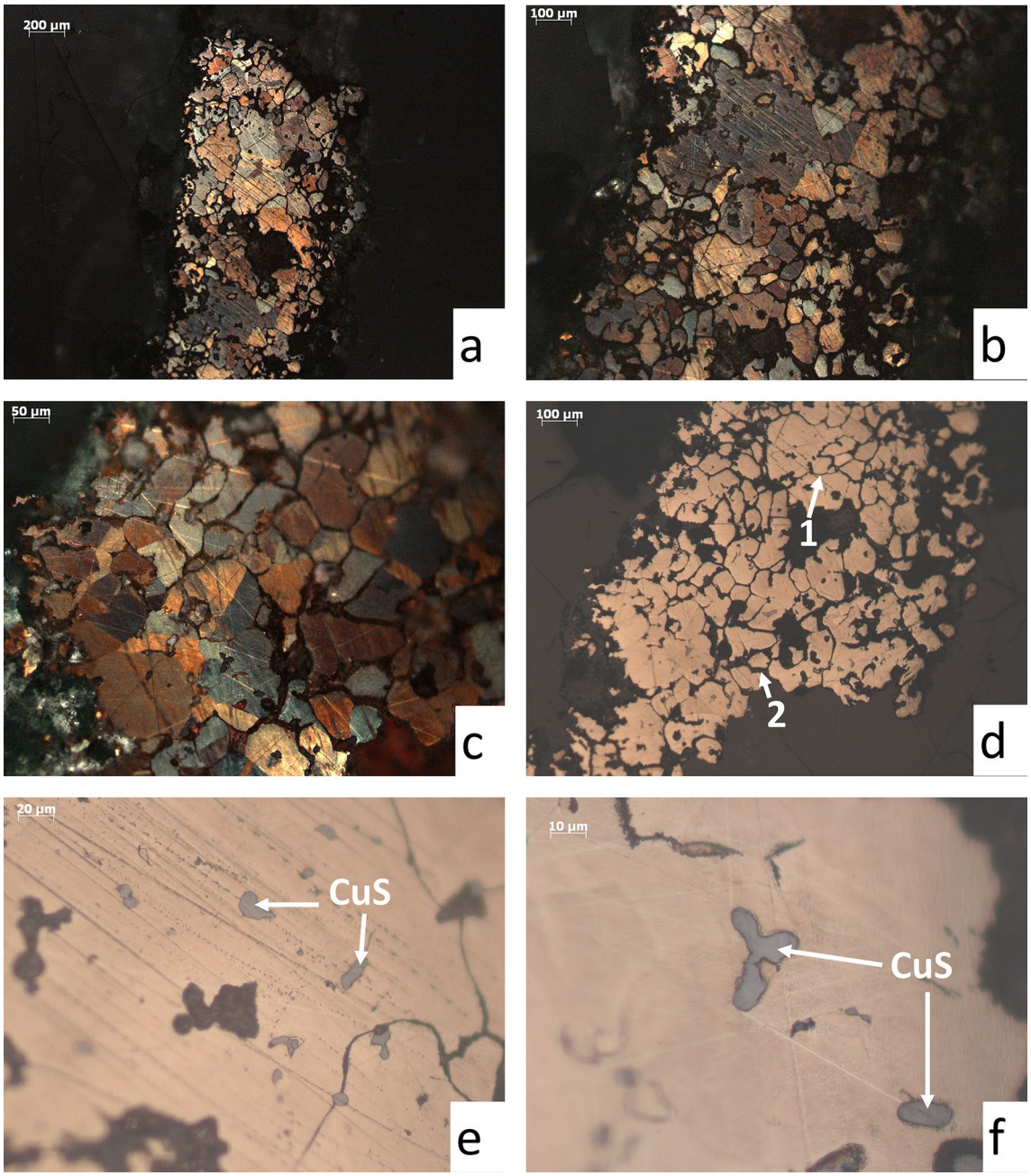

Fig. 5 Optical micrographs of the Sample 1 taken from the bronze sword. Photos (**a**, **b** and **c**) were made in polarized illumination. Recrystallized grain structure with duplex grain size can be seen on the micrographs. Photos (**d**, **e** and **f**) were made in bright field illumination. Corrosion product situated at the grain boundary. Copper-sulphide inclusions are inside the grains and the corrosion product

tin enrichment can be measured in the corrosion product. The enrichment of tin in the corrosion process is a known phenomenon that should be expected. However, here its extent is also significant in comparison with the high tin content of the alloy. Although the local analysis did not detect the silicon and aluminium content, the chemical element maps of Fig. 8 show higher silicon and aluminium concentration. So, the aluminium content can also be linked to the corrosion product.

It can be seen on the chemical element maps that the silicon content is not uniform in the corrosion product. There are areas where a higher silicon amount is detected. This explains why it was not detected in local analysis. It can be clearly seen that the distribution of phosphorus content is correlated with the silicon distribution, so it comes from the same corrosion process as silicon. The sulphur and tin content seem uniformly higher than in the metal matrix. To investigate this, a tin and copper distribution function

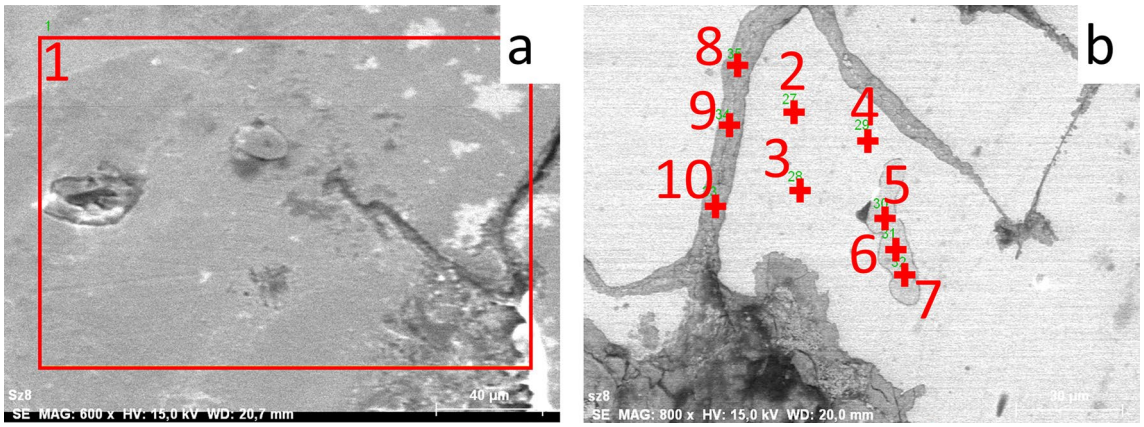

Fig. 6 SEM micrographs of the Sample 1 of bronze sword. Areas of the EDS analysis of the average chemical composition (**a**) and of the local analysis of different phases (**b**) are shown on the photos

Table 2 Results of the EDS analyses of sample 1 taken from the broken grip plate of the bronze sword

Location	C	O	Al	Si	P	S	Fe	Ni	Cu	As	Ag	Sn
1	12.3	8.8	0.2	0.4	0.1	0.1		1.5	67.0	0.2	0.3	9.2
2	11.6	2.7							78.1			7.5
3	10.1	1.7							80.4			7.8
4	9.3	1.4							80.6			8.8
5	10.6	1.7				17.5			70.3			
6	12.8	2.5				16.8			67.9			
7	10.3	1.5				16.8			71.4			
8	16.4	18.4			0.9	0.6	0,1		34.8	0.1		28.7
9	18.6	21.3			0.8	0.4	0,2		32.7			26.0
10	19.4	24.8			0.6	0.2	0,6		30.5	0.2		23.8

The location of the analyses is indicated in Fig. 6

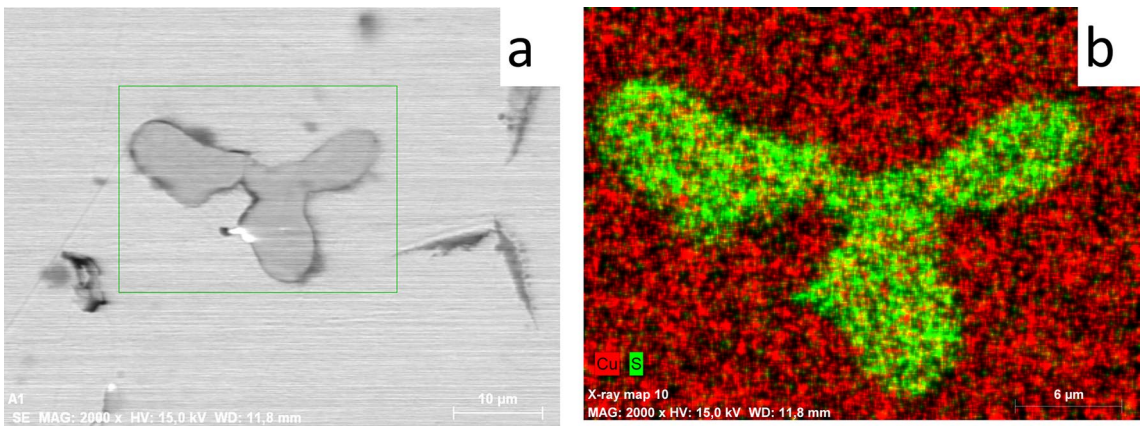

Fig. 7 The chemical element map of the dendritic inclusion on Fig. 5f based on EDS analysis. The inclusion is copper sulphide. The small bright phase which is attached to the inclusion is lead

was measured nearly perpendicular to the grain boundary to the corrosion product, which is shown in Fig. 9. The transition from the metal matrix is diffuse, however, the tin content rises sharply in the corrosion product. What is interesting from the diagram is that the tin content also varies significantly in the bronze matrix in addition to the corrosion product.

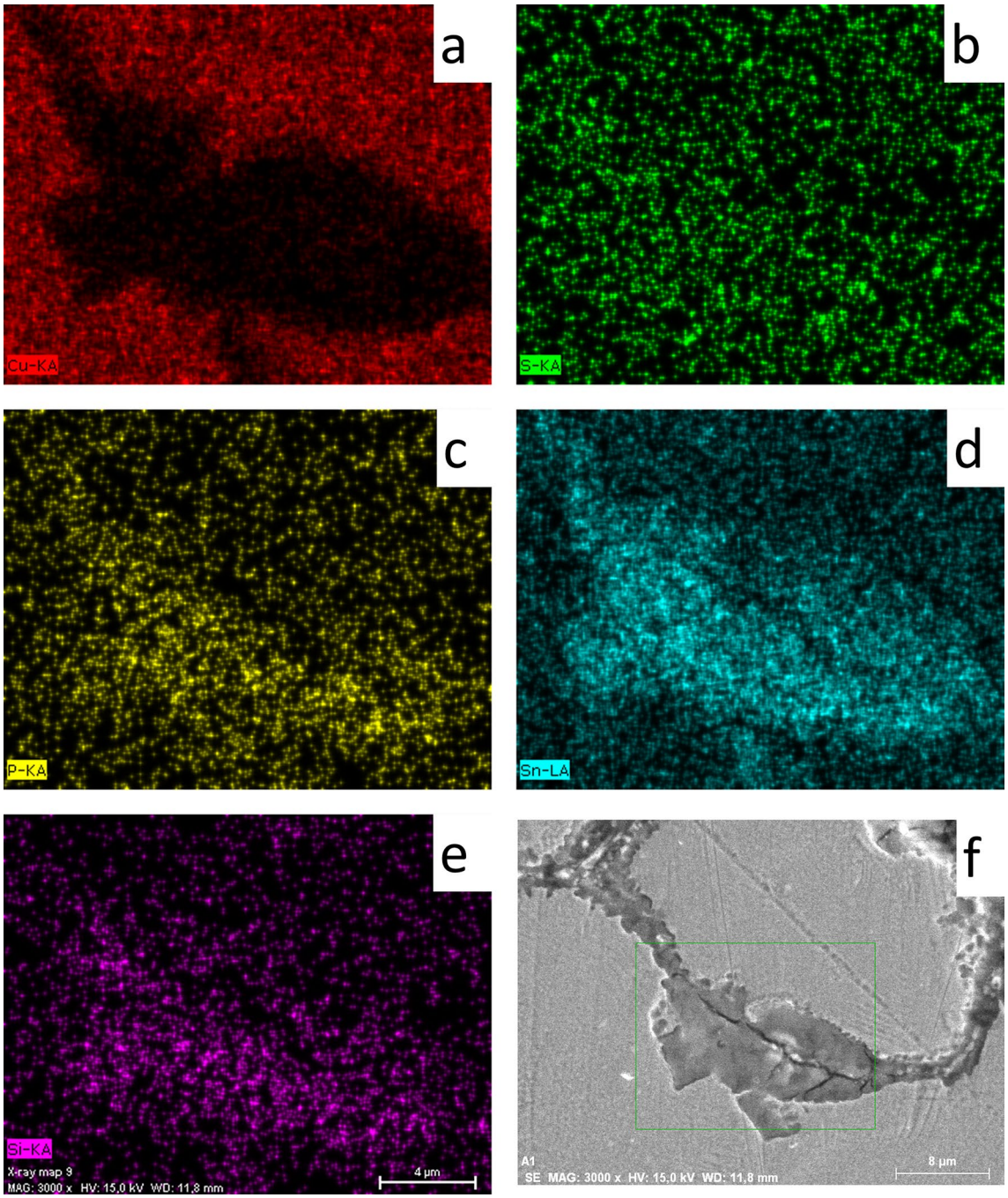

Fig. 8 The chemical element distribution maps taken from the corrosion product on grain boundary by SEM–EDS. The corrosion product contains less copper but significantly more tin than the metal matrix inside the grains. Next to these the phosphorus and silicon content also increases in some areas of the corrosion product

The corrosion product contains a significant amount of tin compounds in addition to copper compounds. It also contains small amounts of iron, phosphorus, sulphur, and silicon certainly in the form of compounds. It is necessary to take this into account, the phosphorus, silicon, and aluminium content of the measured average composition on area of interest by SEM is due to the corrosion product.

Sample 2 of the Bronze Sword

The previous sample differs from the blade fragment both in its alloy and in its microstructure. For this reason, the grip plate was sampled from another location. Figure 10. shows the microstructure of the sample. This sample also has a dendritic microstructure, which suggests casting as

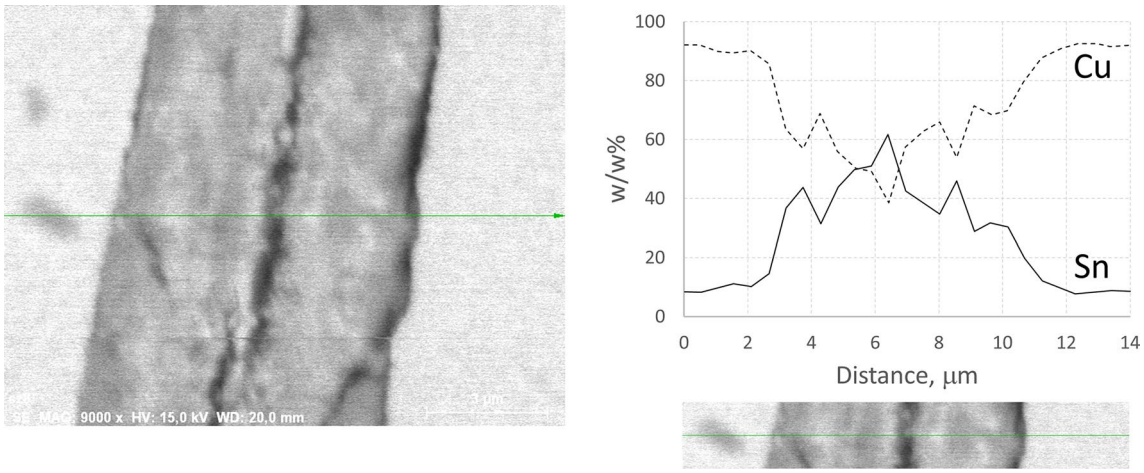

Fig. 9 Copper and tin distribution along a line through the corrosion product on Fig. 8. measured by SEM–EDS. The plot clearly shows the tin enrichment in the corrosion product

a manufacturing technique (Fig. 10a and b). The section shows that the entire cross-section is affected by corrosion (Fig. 10b), which should be considered when the results are evaluated. The dendrite arm spacing is ~ 25 µm, as in the case of the blade fragment (Fig. 10d). The dendrites are not so strongly articulated, but the grain structure is more visible in polarized light than in the case of the blade fragment (Fig. 10c).

The average grain size is ~ 120 µm. Considering these data, the rate of crystallization, as well as the rate of cooling was slower in this part. This is explained by the geometry and the greater metal mass, compared to the blade fragment. Inclusions can be clearly distinguished from the corrosion product in the high magnification micrographs (Fig. 10e and f). At least 2 types of inclusions can be identified on the photos. Dark gray inclusions are copper sulphide inclusions. It was found with two types of morphology, dendritic and spherical. Next to these, lead inclusions can be seen in a light grey colour. This sample contains far fewer lead inclusions than the blade fragment. The larger phases visible between the dendrite arms and following the contour of the dendrite arms are also a corrosion product in this sample. SEM–EDS analysis was performed in areas to determine the average composition (Fig. 11). The results of the EDS analysis are shown in Table 3.

The alloy is almost completely identical to the previous sample. Its tin content is high (~ 7.5 wt.%). In addition, the lead distribution is inhomogeneous and lead inclusions are found in little amount in the section. The nickel and arsenic content must be highlighted, which can also be detected in the other sample. No silver content was detected in the studied areas. Silver was measured in very small quantities in Sample 1. The different state of the corrosion may be the cause of this deviation. Antimony was not detected in this section either. The appearance of silicon, aluminium, phosphorus, and iron is due to the existence of corrosion product, hence the corrosion processes. Sulphur is also found in sulphide inclusions and in the corrosion product according to previous test results.

This sample also suggests that the blade fragment is not made from the same alloy as the sword. The tin content differs significantly from the blade fragment. Although the blade fragment has a similar base copper alloy, it has a significantly lower tin content and a higher lead content than the alloy of the sword. Additionally, no antimony could be detected in the sword material. In addition, this sample prove the premise that the sword itself was made by casting. However, based on Sample 1, either the last manufacturing steps were carried out while the sword was still warm, or where the previous sample was taken, the material of the sword was slightly deformed when it was taken out of the mould.

The Rivet

The grip plate of the sword and the place of the cross-guard are designed in such a way that the grip and the guard element can be fixed there with rivets. The holes in the grip plate and the bronze rivets show this. Nothing of the grip part remains to reconstruct it. But one of the rivets could be removed for inspection. The rivet was examined in its entire cross-section. Optical microscopy images are shown in Fig. 12. The section is significantly affected by the effects of corrosion, although the grain structure is clearly visible. The micrographs show recrystallized structure with a uniform medium grain size (~ 50 µm) (Figs. 12a and b). Dark grey copper sulphide inclusions are mainly at the grain boundaries. In addition to inclusions, a corrosion product is also found in this sample at the grain boundaries (Fig. 12c and d).

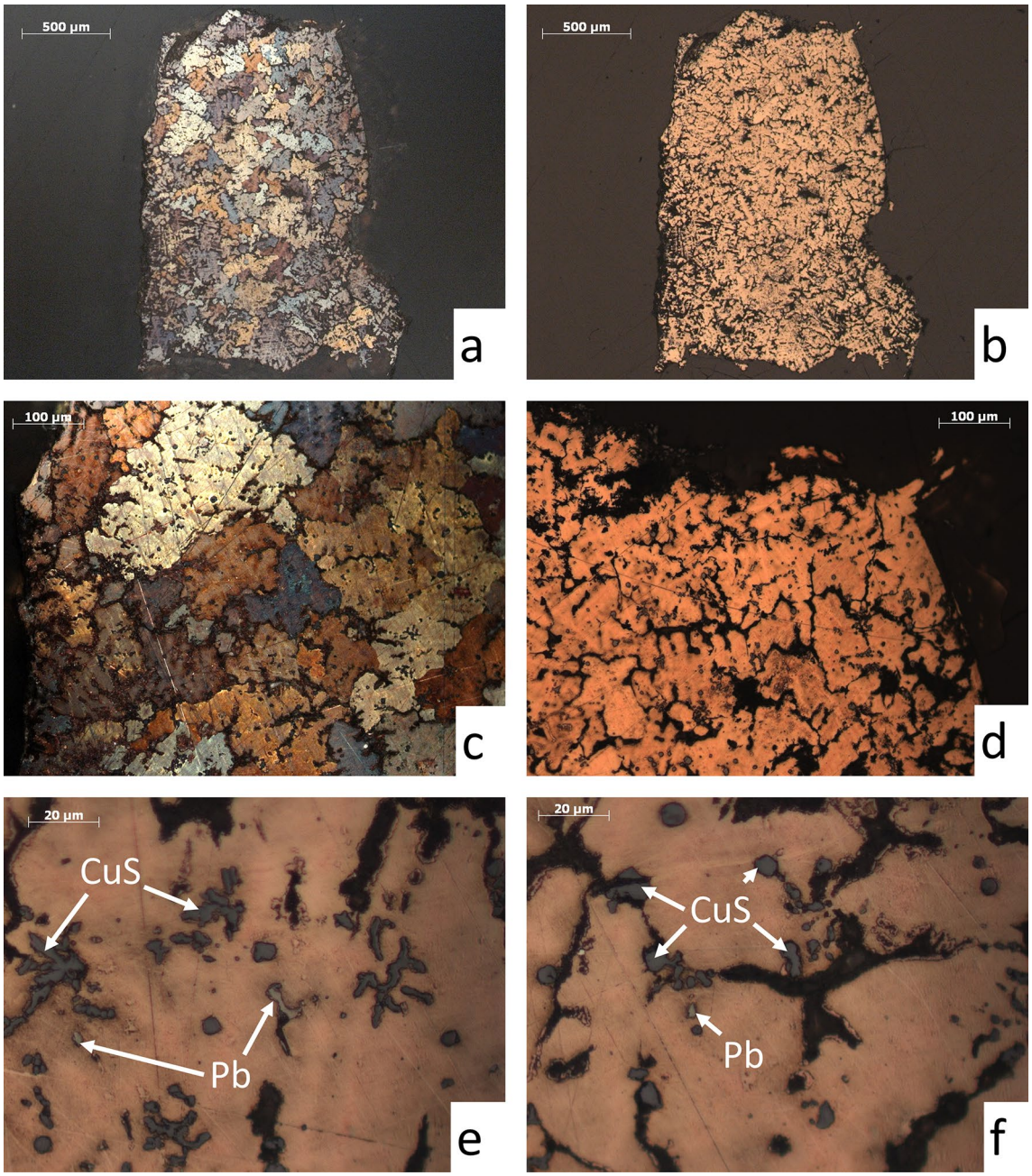

Fig. 10 Optical microscopic images of sample 2 taken from the handle plate of the bronze sword. Dendritic structure can be seen on the photos. The (**a**, **b**, and **c**) images were made in polarized illumination, while the (**d**, **e**, and **f**) micrographs were taken in a bright field illumination. The grain structure formed by the dendrites is clearly visible under polarized light. A corrosion product and various inclusions can be seen in some places between the dendrite arms in bright field images

SEM–EDS test was performed to analyse the composition (Fig. 13). In terms of the composition of the rivet, it is bronze with a medium tin content (4.8 wt.%) (Table 4). In addition to the tin content, the rivet also contains a significant amount of arsenic. A minimum amount of silver can be detected, but no antimony content is measured. Nickel is contained in a larger amount by the corrosion product on the grain boundary however the alloy itself does not contain it. This suggests that the alloy is not identical to the material of the sword, which is caused not only by the difference in the tin content. Due to the smaller tin content, the estimated strength of the material of the rivet is lower, it is more malleable [42, 43]. It corresponds to the application as a rivet. When analysing the corrosion product, tin is significantly enriched in it. In addition, the titanium, manganese, iron and in this case nickel content can also be associated

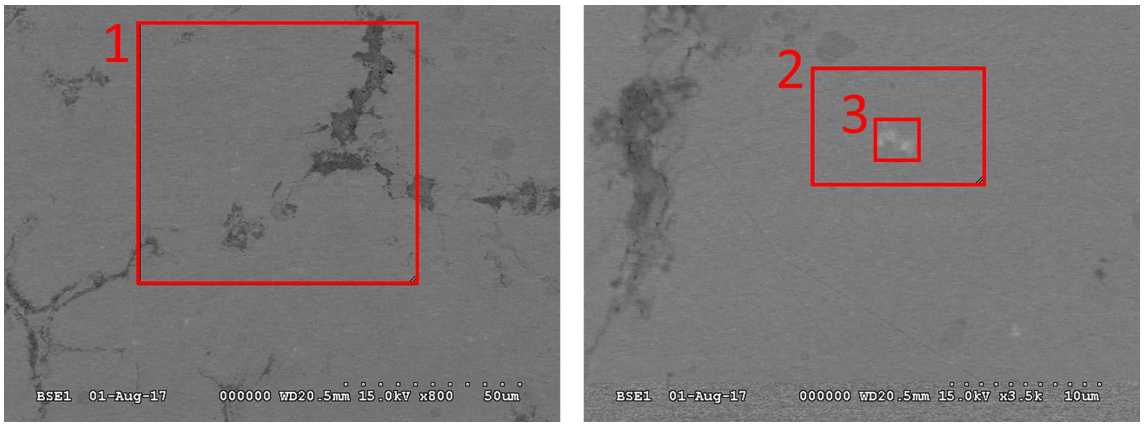

Fig. 11 SEM images of sample 2 taken from the grip plate of the bronze sword and the areas of EDS analysis

Table 3 Results of the EDS analyses of sample 2 taken from the grip plate of the bronze sword

Location	C	O	Al	Si	S	Mn	Ni	Cu	As	Sn	Pb
1	2.5	1.1	0.4	0.4	0.8		1.0	85.2	1.2	7.5	
2	1.5	0.2			0.6	0.4	1.0	85.8		8.7	1.8
3	2.5				0.3	0.3	0.8	83.6	0.9	7.5	4.2

The location of the analyses is indicated in Fig. 11

with a corrosion product. The average composition analysis detected a minimum amount of lead content. Lead is found in the corrosion product as an independent phase.

Bronze Dagger

The bronze dagger is corroded to such an extent that the sample contains only a small number of metallic parts (Fig. 14a). The metallic area visible in the section is unsuitable for determining the manufacturing technique (Fig. 14b). The local composition of the metallic part can be investigated by SEM–EDS analysis. During the evaluation the effect of corrosion must be taken into account, for example the enrichment of elements. In addition, the corrosion product can also be excited during the test which could modify the results (Fig. 14c). With these the tin content of metallic grains is high at 11.8 wt.%. In addition, a significant (2.2 wt.%) arsenic content can be measured. Silver and antimony were not detectable. Nickel in relatively high quantities: 2.6 wt.% can be measured, although in the case of the rivet it is not clear whether it is contained in the metal or in the corrosion product. Sulphur was detected in the amount of 1.5 wt.%. Between the metallic particles and in some places in the particle itself, copper sulphide inclusions can be seen (Fig. 14d). The measured sulphur content can be attributed to these inclusions. No lead could be detected. In addition to copper sulphide inclusions, small sized lead inclusions are also found in this sample (Fig. 14d). The size and quantity of lead particles are so small that these really do not manifest themselves in the test results of the metallic grains. The remaining detected elements (Al, Si, P, Cr, Fe) are a consequence of the excitation of the corrosion product.

In terms of tin content, even if the tin is enriched in metallic grains, the dagger is made of an alloy with a high tin content. In terms of arsenic and nickel, it can also be considered to be a similar alloy to sword. Unfortunately, due to strong corrosion, a more detailed comparison cannot be made between the two objects. However, it appears that the sword and dagger are made of a higher hardness, higher strength high-tin alloy, which is supposed based on their use. For each object have an as cast or annealed state. Tin content is one of the determinants in terms of strength based on the literature data. In the case of blade fragment and rivet can be estimated a tensile strength of ~ 350 N/mm2 in terms of tin content of 5 wt.%. In the case of sword and dagger it is more than ~ 410 N/mm2. Lead content does not significantly alter the strength of the blade fragment. The strength is also modified by other constituents of course. For example, the amount of arsenic in the case of dagger is further increases the strength of the alloy.

Summary

Among other objects, the collection of artifacts in Vértesszőlős includes a fragmented bronze sword, a blade fragment, and a bronze dagger. All these objects can be

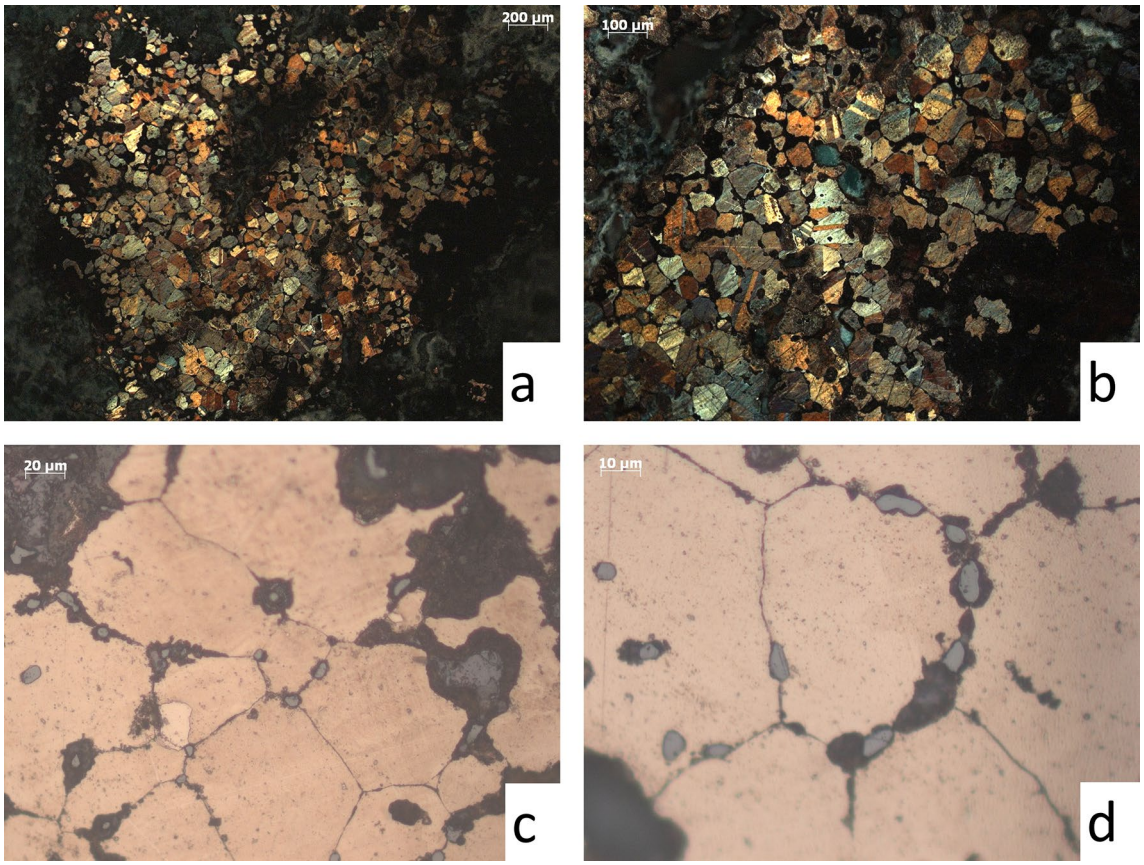

Fig. 12 Optical microscopic images of the sample of the rivet. The a and b photos were taken in polarized illumination. Fine, uniform recrystallized grain structure can be seen. The c and d shots were taken in bright field illumination. Corrosion product and copper sulfide inclusions on the grain boundaries show by the micrographs

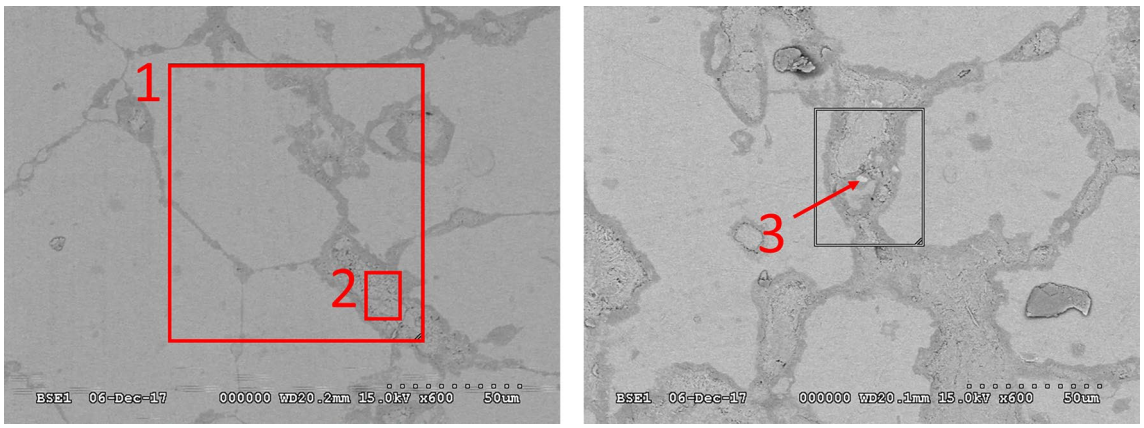

Fig. 13 SEM micrographs of the rivet sample. The places of the EDS analysis are signed in the photos

associated with the Late Bronze Age. The purpose of the study is to present a metallographic examination and description of the objects. To do this, samples of the objects were taken, which were examined by optical microscope and the SEM–EDS method.

The blade fragment is bronze alloy with medium tin and high lead content. In addition, nickel, arsenic, silver, and antimony were detected in small quantities. The bronze sword, for which the tip was this blade fragment, was made by casting. Presumably therefore its lead content is high.

Table 4 The results of EDS analysis of the rivet

Location	C	O	Mg	Ca	S	Ti	Mn	Fe	Ni	Cu	As	Ag	Sn	Pb
1	2.5	1.5			0.1	1.7	2.4	2.6		81.2	2.7	0.1	4.8	0.3
2	3.1	3.9			0.1	1.7	2.1	2.2	4.0	69.9	1.9	0.1	8.5	0.1
3	9.7		0.5	2.4			4.7			15.1	1.4			66.3

The locations of the tests are showed in Fig. 13. The data presented in w/w%

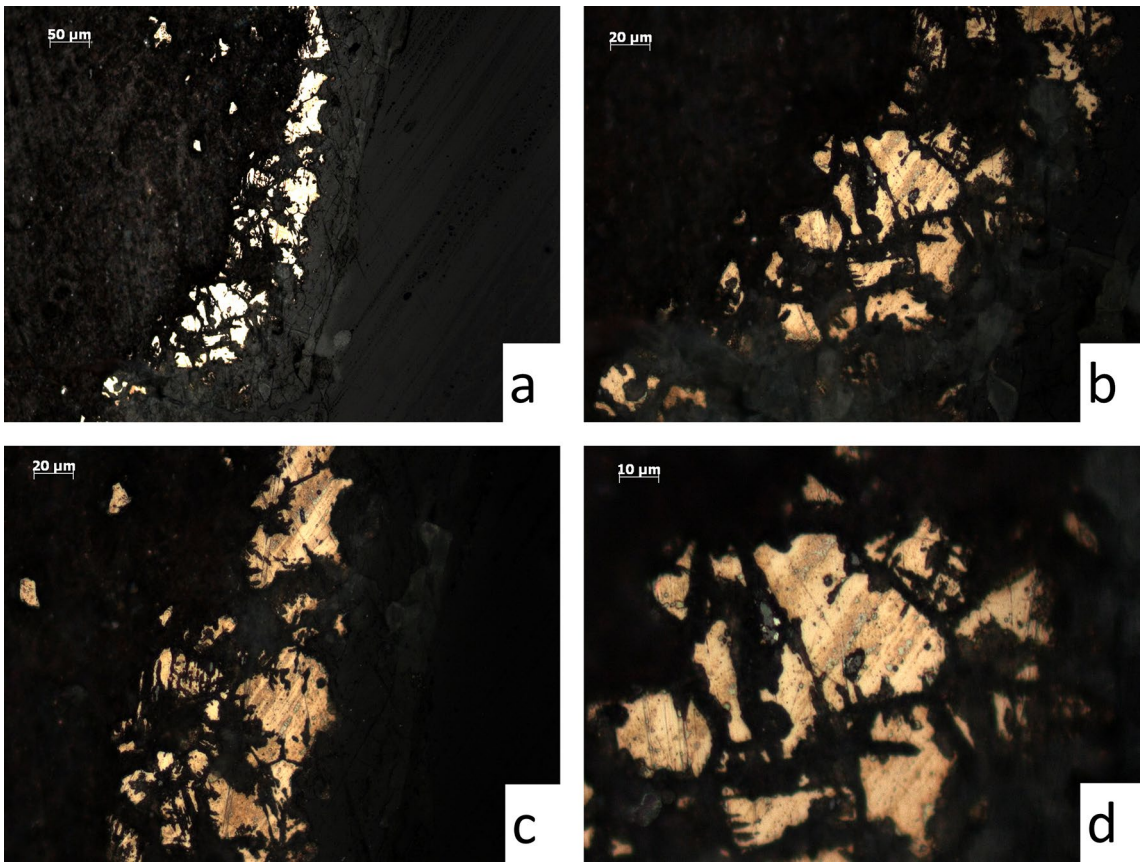

Fig. 14 Bright field optical micrographs of the sample of the dagger. Just a few metallic particles can be seen in the sample. Copper-sulphide inclusions can be observed between the metallic particles. Small lead inclusions are attached to the sulphide inclusions

In terms of the amount of tin, its content determined the mechanical properties of the alloy. It resulted in a moderately hard sword. The microstructure suggests that after casting, the sword cooled rapidly. In addition to copper sulphide, lead inclusions, copper-tin intermetallic phases due to micro-segregation are also found in the microstructure.

The bronze sword is made of an alloy which is significantly different from the broken sword end. The material of the sword has a high tin content and little lead can be detected. Nickel and arsenic can be measured in the alloy. Silver content was also measured in one of the samples. The distribution of arsenic and silver is inhomogeneous in the alloy. However, antimony cannot be detected in the samples. It shows that the blade fragment is not the broken tip of the sword. That piece belongs to another sword. The sword was also made by casting, its cooling rate based on the secondary dendrite arm distance was slower than in the case of the blade fragment. In a sample taken from the edge of the handle plate, recrystallized grains of duplex size were found. This suggests a small degree of hot deformation. Given the nature of the object, it cannot be decided whether a metal forming took place here, or whether the sword was taken out of the arm mould in a way that resulted in a small deformation. Mostly copper sulphide inclusions were found in the microstructure of the sword. Lead is found in small quantities, in small inclusions. These tiny inclusions are typically observed attached to copper sulphide inclusions. The tin content in this case also significantly determines the properties of the alloy. Considering this, we get a hard material that is suitable for sword use.

In the sword there were rivets in the part between the handle plate and the blade, in the place of the guard. A rivet was removed from it. The rivet bronze material has a medium tin content. In addition, it contains only little arsenic. Silver was detectable, but in negligible quantities. The rivet is not made of the material of the sword. In addition, the smaller content of tin leads to less hardness, strength. However, the alloy is more ductile, making it suitable for rivets.

In the case of the bronze dagger, the sample contained just few metallic grains. The dagger is significantly corroded. From the microstructure, the manufacturing technique could not be identified. Given the shape, size, and nature of the object, casting can be assumed. Compared to the sword, this is also indicated by the measurably high tin content. However, the evaluation of the test results of the dagger requires care due to the strong corrosive effect. The high content of tin in this case also resulted in a dagger of high strength, high hardness.

The test results of sword fragments and dagger are an essential stage in the examination program of the site, as it adds new results in terms of the classification of alloys and processing techniques for such important objects as bronze weapons.

Funding Open access funding provided by University of Miskolc.

References

1. G. Pál, J. CsehKis, Prehistoric, roman and Árpád Age excavations on the outskirts of Vértesszőlős. A preliminary report of Vértesszőlős 92/2 site's excavation. Tatabányai Múzeum Évkönyve. **3**, 5–19 (2013)
2. G. Kulcsár, V.G. Szabó, V. Kiss, G. Váczi (eds.), *State of the hungarian bronze age*. (Prehistoric Studies II, 2017)
3. T. Horváth, J. Cseh, P. Barkóczy, L. Juhász, S. Gulyás, Z. Bernert, Á. Buzár, A double burial of the Baden culture from Tatabánya-Delphi (northern Transdanubia, Hungary): a case study of the Dentalium beads of the Baden culture and their interpretation. Quat. Int. **539**, 78–91 (2020)
4. V. Kiss, Transformations of metal supply during the Bronze Age in the Carpathian Basin. Hung. Hist. Rev. New Ser. Acta Hist. Acad. Scientiarium Hung. **9**, 315–330 (2020)
5. V. Kiss, A. Czene, M. Csányi, J. Dani, S. Fábián, K. Fischl, D. Gerber, J.I. Giblin, T. Hajdu, K. Köhler, E. Melis, B.G. Mende, R. Patay, G. Szabó, A. Szécsényi-Nagy, V. Szeverényi, G. Kulcsár, Methods and opportunities in the research of bronze age communities: the outcomes of the bioarchaeological research programme of the momentum mobility research group (2015–2020). Hung. Archaeol. **10**, 30–42 (2021)
6. B. Török, P. Barkóczy, Á. Kovács, T. Ferenczi, K. Fischl, Examination of surface layer of Bronze Age pick of Hajdúsá mson type. Surf. Eng. **29**, 164–168 (2013)
7. T. Horváth, 4000–2000 BC in Hungary: the age of transformation. Annales Univ. Apulensis. Ser. Hist. **20**, 51–112 (2016)
8. V. Kiss: Middle Bronze Age Encrusted Pottery in western Hungary, VARIA ARCHAEOLOGICA HUNGARICA XXVII, Archeolingua, 2012
9. F. Gogaltan: Bronze Age Chronology in The Carpathian Basin Proceedings of the International Colloquium from Târgu Mureş in: R. E. Németh, B. Rezi Ed.: Bronze Age Chronology in the Carpathian Basin. Proceedings of the International Colloquium from Târgu Mureş 2–4 October 2014, Cluj-Napoca,. pp. 53–95., 2016
10. Z. Czajlik, K. G. Sólymos: Analyses of ingots from Transdanubia and adjacent areas. In: E. Jerem, K. T. Bíró, E. Rudner Ed.: Archaeometry 98. Proceedings of the 31st Symposium Budapest, April 26 - May 3 1998, Vol. II, BAR International Series 1043 (II), pp. 317–325, 2002
11. M. Mödlinger, P. Trebsche, Archaeometallurgical investigation of a Late Bronze Age hoard from Mahrersdorf in Lower Austria. J. Archaeol. Sci. Rep. **33**, 1–15 (2020)
12. O. Oudbashi, P. Davami, Metallography and microstructure interpretation of some archaeological tin bronze vessels from Iran. Mater. Charact. **97**, 74–82 (2014)
13. Ilon Gábor: THE GOLDEN TREASURE FROM SZENT VID IN VELEM The Costume of a High-Ranking Lady of the Late Bronze Age in the Light of New Studies. Series Minor 36, Archeolingua, 2015
14. P. Sureda, J. Deyà, P. Galera, M. Murillo-Barroso, B. Salvà-Simonet, Emblematic objects for societies in transition. An archaeological and archaeometric study of the sword of Serral de ses Abelles (Puigpunyent, Mallorca). J. Archaeol. Sci. Rep. **40**(Part A), 1–14 (2021)
15. M. Mödlinger, P. Piccardo, Z. Kasztovszky, I. Kovács, Z. Szőkefalvi-Nagy, G. Káli, V. Szilágyi, Archaeometallurgical characterization of the earliest European metal helmets. Mater. Charact. **79**, 22–36 (2013)
16. A. Čivilytė, E. Duberow, E. Pernicka, K. Skvortzov, The new Late Bronze Age hoard find from Kobbelbude (former Eastern Prussia, district Fischhausen) and the first results of its archaeometallurgical investigations. Archaeol. Anthropol. Sci. **9**, 755–761 (2017)
17. A. Giumlia-Mair, E.J. Keall, A.N. Shugar, S. Stock, Investigation of a copper-based hoard from the megalithic site of al-midamman, yemen: an interdisciplinary approach. J. Archaeol. Sci. **29**(2), 195–209 (2002)
18. T.L. Kienlin, *Traditions and Transformations: Approaches to Eneolithic (Copper Age) and Bronze Age Metalworking and Society in Eastern Central Europe and the Carpathian Basin. BAR International Series 2184* (Archaeopress, 2010)
19. A.M. Jones, J. Gossip, H. Quinnell (eds.), *Settlement and metalworking in the Middle Bronze Age and beyond: New evidence from Tremough*. (Sidestone press, 2015)
20. H. WrobelNørgaard, Metalcraft within the Nordic Bronze Age: combined metallographic and superficial imaging reveals the technical repertoire in crafting bronze ornaments. J. Archaeol. Sci. **64**, 110–128 (2015)
21. J. Ling, E. Hjärthner-Holdar, L. Grandin, Z. Stos-Gale, K. Kristiansen, A.L. Melheim, G. Artioli, I. Angelini, R. Krause, C.

Canovaro, Moving metals IV: swords, metal sources and trade networks in Bronze Age Europe. J. Archaeol. Sci. Rep. **26**, 1–34 (2019)
22. J. Wadsworth, Archeometallurgy related to swords. Mater. Charact. **99**, 1–7 (2015)
23. V. Kiss, The study of gold, copper and bronze artefacts until the Middle Bronze Age–current questions of archaeometallurgy. Archeometriai Műhely. **2**, 61–74 (2012)
24. H. Wei, W. Kockelmann, E. Godfrey, D.A. Scott, The metallography and corrosion of an ancient chinese bimetallic bronze sword. J. Cult. Herit. **37**, 259–265 (2019)
25. G. Szabó: Archaeometallurgical investigation of the LBA bronze objects in the Carpathian Basin. In: E. Jerem, K. T. Bíró, E. Rudner Ed.: Archaeometry 98. Proceedings of the 31st Symposium Budapest, April 26 - May 3 1998, Vol. II, BAR International Series 1043 (II), pp. 481–490, 2002
26. L. Dumont, V. Dupuy, T. Nicolas, C. Pelé-Meziani, G.D. Mulder, The protohistoric sword from Le Gu´e-de-Velluire (Vend´ee, France): a pasticcio's history unveiled by archaeometrical research. J. Archaeol. Sci. Rep. **34**, 1–8 (2020)
27. D.A. Scott, R. Schwab, *Metallography in Archaeology and Art* (Springer, 2019)
28. G. Szabó, Practical and ethical issues of archaeometallurgic research. Archeometriai Műhely. **2**, 111–122 (2010)
29. D.A. Angel, T. Miko, F. Kristaly, M. Benke, Z. Gacsi, G. Kaptay, Complex Avrami kinetics of TiB2 transformation into TiB whiskers during sintering of Ti-TiB2 nanocomposites. J. Alloy. Compd. **894**, 1–8 (2022)
30. G. Szabó, Recent advances and nes questions of archaeometallurgical research in the Carpathian Basin at at he beginning of the 21st Century, with special emphasis on the change in the social background of bonze and iron artefacts. Archeometriai Műhely. **9**, 75–96 (2012)
31. C. Chen, L. Zhang, S. Wright, S. Jahanshahi: Thermodynamic Modelling of Minor Elements in Copper Smelting Process. In: Sohn International Symposium Advanced Processing of Metals and Materials Volume 1 - Thermo and Physicochemical Principles: Non-Ferrous High-temperature processing Edited by F. Kongoli and R.G. Reddy TMS (The Minerals, Metals & Materials Society), pp. 335–348., 2006
32. L. Klemettinen, K. Avarmaa, H. O'Brien, P. Taskinen, A. Jokilaakso, Behavior of tin and antimony in secondary copper smelting process. Minerals. **9**, 1–16 (2019)
33. G. Szabó, P. Barkóczy, S. Gyöngyösi, Z. Kasztovszky, G. Káli, Z. Kis, B. Maróti, V. Kiss, The possibilities and limitations of modern scientific analysis of Bronze Age artefacts in Hungary. Archeometriai Műhely. **16**, 1–12 (2019)
34. D. Berger, Q. Wang, G. Brügmann, N. Lockhoff, B.W. Roberts, ErnstPernicka: the Salcombe metal cargoes: new light on the provenance and circulation of tin and copper in Later Bronze Age Europe provided by trace elements and isotopes. J. Archaeol. Sci. **138**, 105543 (2022)
35. G. Artioli, I. Angelini, P. Nimis, I.M. Villa, A lead-isotope database of copper ores from the South-eastern Alps: a tool for the investing action of prehistoric copper metallurgy. J. Archaeol. Sci. **75**, 27–39 (2016)
36. J.A. Stephens, M.N. Duceab, D.J. Killick, J. Ruiz, Use of non-traditional heavy stable isotopes in archaeological research. J. Archaeol. Sci. **127**, 1–20 (2021)
37. M. Mödlinger, E. Godfrey, H. Postma, P. Schillebeeckx, W. Kockelmann, Neutron analyses of eight Bronze Age swords from Austria: the question of 'stabbing' or 'cut-and-thrust' weapons. J. Archaeol. Sci. Rep. **33**, 1–13 (2020)
38. M. Mödlinger, E. Godfrey, W. Kockelmann, Neutron diffraction analyses of Bronze Age swords from the Alpine region: Benchmarking neutron diffraction against laboratory methods. J. Archaeol. Sci. Rep. **20**, 423–433 (2018)
39. F. Grazzi, A. Brunetti, A. Scherillo, M.E. Minoja, G. Salis, S. Orrù, A. Depalmas, Non-destructive compositional and microstructural characterization of Sardinian Bronze Age swords through Neutron Diffraction. Mater. Charact. **144**, 387–392 (2018)
40. N. Nerantzis, Shaping bronze by heat and hammer: an experimental reproduction of minoan copper alloy forming techniques. Mediter. Archaeol. Archaeom. **12**, 237–247 (2010)
41. H. Okamoto, M.E. Schlesinger, E.M. Mueller (eds.), *ASM Handbook Volume 3: Alloy Phase Diagrams*. (ASM International, 2016)
42. ASM International: ASM Handbook Volume 2: Properties and Selection: Nonferrous Alloys and Special-Purpose Materials, ASM International, 1990
43. Wolf Mária ed.: Hejőkeresztúr-Vizekköze, A tatárjárás régészeti emlékei 1. Opitz Archaeologica, vol. 22 Budapest, 2022
44. I. Ringer, P. Barkóczy, Á. Kovács, L. Pásztor, Examination of the microstructure of the findings from cannon foundry sárospatak. Mater. Sci. Forum. **729**, 7–12 (2013)
45. A. Berta, B. Török, M. Tóth, P. Barkóczy, Á. Kovács, K. Fintor, Archaeometallurgical examination of finds from medieval bell casting foundries in Hungary, in *Archaeometallurgy in Europe IV*. ed. by I. Montero-Ruiz, A. Perea (Consejo Superior de Investigaciones Científicas (CSIC), 2017), pp.259–267